Design of Channel Coded Heterogeneous Modulation Physical Layer Network Coding

Haoyuan Zhang, *Student Member, IEEE*, and Lin Cai, *Senior Member, IEEE*

***Abstract*—In a two-way relay channel network (TWRC), the integration of channel coding into symmetric physical layer network coding (PNC) has been well studied, where both sources use exactly the same channel coding and modulation schemes and the relay decodes and reencodes the codewords obtained from the superimposed signals. How to integrate the channel coding into heterogeneous modulation PNC (HePNC), where the sources apply different modulations, is an open issue. In this paper, we propose a channel coded HePNC (CoHePNC) scheme under asymmetric TWRC. For repeat-accumulate (RA) codes applied at the sources, a full-state sum-product decoding algorithm is proposed which enables the relay to decode the superimposed signals from the sources to the raw decoding results firstly, and then re-encode and obtain the network-coded codewords by mapping the raw decoding results according to the proposed bit-level mapping functions. We further optimized the bit-level mapping functions according to the two source-relay channel conditions. Extensive simulation results demonstrated that the proposed CoHePNC outperforms the existing channel coded PNC schemes in terms of the relay decoding error rate and the end-to-end bit error rate under asymmetric TWRC scenarios.**

***Index Terms*—Channel coding, heterogeneous modulation, physical layer network coding, sum product decoding.**

I. Introduction

TWO-way relay channel (TWRC) studied how to efficiently exchange information between two sources through a relay. The physical layer network coding (PNC) protocol proposed in [1], [2] enables the concurrent transmissions from the sources, where the network-coded information containing the necessary information to recover the source data, are extracted form the superimposed signals at the relay in the multiple access (MA) stage and then be broadcast back to both sources in the broadcast (BC) stage. Each source can extract the other's information by decoding the network-coded information and eliminating its own information. PNC increases the spectrum efficiency significantly comparing to the traditional TDMA and network coding protocols [3]–[11].

How to integrate the channel error control coding into PNC to guarantee the reliable transmission is an important issue. Depending on whether the relay decodes the codewords from the sources in the superimposed signals, channel coded PNC can be classified into two categories, including the end-to-end coding and link-to-link coding [3]. In the end-to-end coding, the relay processes the superimposed signals in a symbol-level without further decoding the superimposed codewords. In other words, the channel coding and decoding are processed at both sources only. Thus, the end-to-end coding suffers from the noise accumulation at the relay, which further impacts on the end-to-end bit error rate (BER) performance in the BC stage. In the link-to-link coding [12]–[23], the relays decode the superimposed signals to try to correct the errors happened in the MA stage. Thus, link-to-link coding outperforms the end-to-end coding in terms of the end-to-end BER.

PNC is mostly researched in the symmetric TWRC scenario [12]–[23], where the two source-relay channel conditions are similar. Thus, the same channel coding and modulation schemes can be applied by both sources. However, in the asymmetric TWRC scenario, where two source-relay links have quite different channel conditions, which is more practical in realistic, the traditional symmetric PNC designs are far from optimal. Several schemes of heterogeneous modulation physical-layer network coding (HePNC) targeting for asymmetric TWRC are proposed [24]–[30], where different modulations can be applied by the sources and a non-equivalent data exchange ratio between them can be supported. However, all of them operate on a symbol-level and end-to-end coding can be integrated only, i.e., the relay does not decode the superimposed codewords and the network-coded information are obtained from the demodulation results in the symbol-level. How to integrate the channel error control coding into HePNC in a link-to-link coding is still an open issue. The design of link-to-link coding for symmetric PNC is challenging, as the decoding algorithm at the relay is required to be designed in specific according to the coding applied at the sources [12]–[23]. The design of link-to-link coding for HePNC is more challenging due to the asymmetry. Considering the source apply the same channel coding, when the same modulation is applied at the sources, two codewords with the same length are superimposed at the relay. However, when different modulations are applied at the sources, e.g., QPSK and BPSK are applied at source A and B, respectively, when source B has transmitted one codeword, two codewords has been transmitted from source A and superimposed with that codeword from B. Thus, the asymmetry in HePNC further challenges the design of link-to-link coding in HePNC.

In this paper, we focus on integrating the channel error control coding into HePNC in a link-to-link coding, and proposed

Manuscript received April 5, 2017; revised September 5, 2017; accepted October 15, 2017. Date of publication October 25, 2017; date of current version March 15, 2018. The review of this paper was coordinated by Dr. T. Jiang. *(Corresponding author: Lin Cai.)*

The authors are with the Department of Electrical and Computer Engineering, University of Victoria, Victoria BC V8P 5C2, Canada (e-mail: hyuan,cai@uvic.ca).

Color versions of one or more of the figures in this paper are available online at http://ieeexplore.ieee.org.

Digital Object Identifier 10.1109/TVT.2017.2766209

channel coded heterogeneous modulation physical-layer network coding (CoHePNC). CoHePNC arranges two stages, i.e., the multiple access (MA) stage and the broadcast (BC) stage. In the MA stage, both sources A and B encode the source data with the same channel coding and transmit the modulated codewords to the relay R simultaneously with different modulations, which are selected according to the two source-relay channel conditions and the data exchange requirement. The relay receives and decodes the superimposed signals by the proposed decoding algorithm to raw decoding results. A network-coded sequence, which contains the necessary information of two source uncoded data, is constructed by mapping the raw decoding resulting with a proper designed bit-level mapping function. In the BC stage, the network-coded sequence is re-encoded and broadcast to the sources, and each source can extract the other's information by decoding the network-coded sequence and eliminating its own information. Note that the bit-level mapping functions are different from the traditional symbol-level mapping functions [24]–[30]. Briefly speaking, in symbol-level mapping, the network-coded symbols are obtained from the demodulation results. Meanwhile in the bit-level mapping, the network-coded information are obtained from the decoding results, which highly depend on the decoding algorithm design.

The main contributions of this paper are four-fold. First, we proposed and designed CoHePNC which integrates channel error control coding into HePNC in a link-to-link coding. Second, based on the repeat-accumulate (RA) codes applied at the sources, a full-state sum-product decoding algorithm is proposed at the relay, which outperforms the existing decoding solutions in terms of relay error rate (RER) and end-to-end BER under asymmetric TWRC. Third, we designed and optimized the bit-level mapping functions instead of the traditional XOR in the symbol-level, which map the raw decoding results to the network-coded sequence adaptively according to the two source-relay channel conditions. Fourth, we conducted extensive simulations under Gaussian, block fading and fast fading channel conditions, and demonstrated the performance gain of our proposed scheme in terms of RER and BER.

The rest of this paper is organized as follows. The related work is summarized in Section II. Section III introduces the system model and CoHePNC procedure. Section IV presents the design and optimization of CoHePNC. Performance evaluations are presented in Section V, followed by the concluding remarks in Section VI.

II. Related Workd

The majority of work studying how to integrate the channel error control coding into PNC refer to the link-to-link coding. In the link-to-link coding [12]–[23], the relay decodes the codewords from two sources in the superimposed signals and tries to minimize the transmission errors happened in the MA stage. The key and tricky issues are how the relay decodes the superimposed codewords and constructs the network-coded sequence, which contains the necessary information of the uncoded data at both sources, from the decoding results. A primitive link-to-link coding PNC proposed in [12] utilized the property that, given a linear code, the XOR result of two linear codewords is still a valid codeword. Thus, the relay tries to decode the XOR result of the superimposed symbols to clear up the noise in the MA stage. The authors in [13] integrated the RA codes into symmetric PNC by re-designing the sum-product decoding algorithm at the relay. The essence in [13] is to upgrade the message passing in the decoding algorithm from the traditional two-state[1] to three-state,[2] where the state defines how many classifications the decoding results have. The authors in [14] followed this idea and proposed a generalized sum-product decoding algorithm with four-state message, where carrier synchronization is not required. Other variants [15]–[17] studied low-density parity-check (LDPC) codes combining PNC by modifying the sum-product decoding algorithm. The authors in [15] estimated the decoding threshold of the LDPC code and optimized the degree distribution of LDPC. The authors in [16] extended the LDPC decoding algorithm to the log-likelihood-ratio domain, and [17] studied the LDPC performance by removing the symbol-level synchronization requirement. The authors in [18] studied irregular repeat accumulate (IRA) code based on an extension of extrinsic information transfer (EXIT). The authors in [19]–[21] studied the convolutional code with PNC and the authors in [20] studied convolutional and turbo codes under various channel conditions, and the authors in [21] further removed the symbol-level synchronization requirement. Note that the above works only considered that BPSK modulation is applied by both sources, which simplifies the decoding design at the relay compared with higher-order modulation PNC. The authors in [22] studied that QPSK modulation is applied by both sources, following by designing the network-coded sequence with XOR mapping. However, for higher-order modulation PNC design, XOR mapping is not optimal [25]–[27]. The authors in [23] integrated IRA with symmetric PNC where both sources apply QPSK or PAM, but they still considered the symmetric link-to-link PNC only.

In practice, there may not exist a relay to support the symmetric two source-relay channel conditions and the data exchange requirement between two sources may not be equivalent. Thus, heterogeneous modulation PNC designs are necessary. The authors in [24]–[30] focused on the HePNC design in the symbol-level. In [24]–[27], the network-coded symbols are constructed adaptively according to the two source-relay channel conditions. The authors in [28]–[30] focused on optimizing the modulation order of the network-coded symbol. However, the existing HePNC [24]–[30] can only be combined with end-to-end coding, and the design of link-to-link coding HePNC is still an open issue. In this work, we refer the designs in [24]–[30] to be symbol-level HePNC.

In this work, we study how to combine channel error control coding with HePNC in the link-to-link coding. We studied

[1] In traditional hop-to-hop transmission, there are only two-state for the message passing in the sum-product decoding algorithm when BPSK modulation is applied, i.e., either 0 or 1.

[2] As perfect symmetric source-relay channel conditions with carrier synchronization is assumed, three-state is maximal when BPSK is applied by both sources, which is further explained in Sec. IV-B

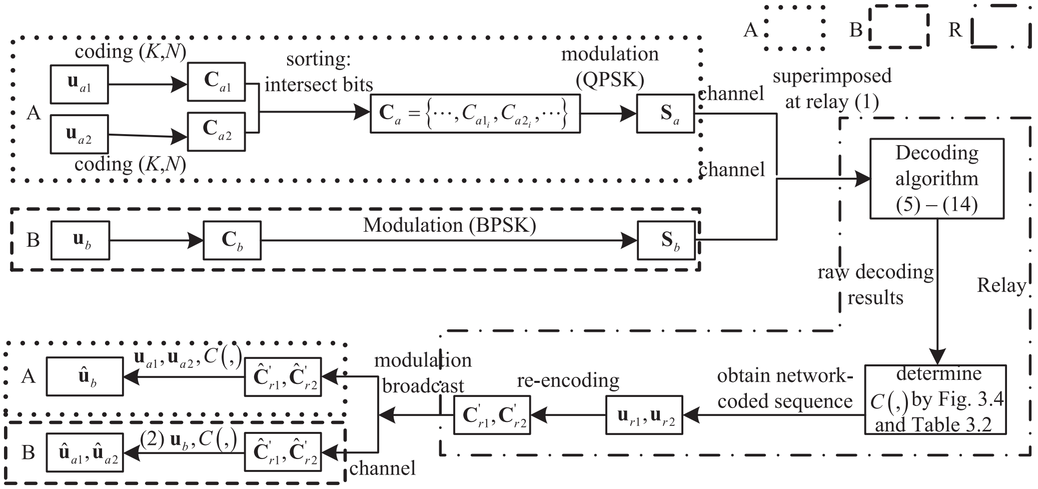
A
B
R
coding (K,N)
$\mathbf{u}_{a1}$
$\mathbf{C}_{a1}$
sorting: intersect bits
modulation (QPSK)
A
$\mathbf{u}_{a2}$
$\mathbf{C}_{a2}$
$\mathbf{C}_a = \{\cdots, C_{a1_i}, C_{a2_i}, \cdots\}$
$\mathbf{S}_a$
coding (K,N)
channel
superimposed at relay (1)
channel
Decoding algorithm (5) – (14)
B
$\mathbf{u}_b$
$\mathbf{C}_b$
Modulation (BPSK)
$\mathbf{S}_b$
raw decoding results
Relay
A
$\hat{\mathbf{u}}_b$
$\mathbf{u}_{a1}, \mathbf{u}_{a2}, C(,)$
$\hat{\mathbf{C}}'_{r1}, \hat{\mathbf{C}}'_{r2}$
modulation broadcast
re-encoding
obtain network-coded sequence
determine $C(,)$ by Fig. 3.4 and Table 3.2
$\mathbf{C}'_{r1}, \mathbf{C}'_{r2}$
$\mathbf{u}_{r1}, \mathbf{u}_{r2}$
B
$\hat{\mathbf{u}}_{a1}, \hat{\mathbf{u}}_{a2}$
(2) $\mathbf{u}_b, C(,)$
$\hat{\mathbf{C}}'_{r1}, \hat{\mathbf{C}}'_{r2}$
channel

Fig. 1. Procedure diagram of integrating channel coding into HePNC in a link-to-link manner.

RA codes and proposed a full-state sum-product decoding algorithm containing full-state message passing jointly with the bit-level adaptive mapping function designs, which are applied to construct the network-coded sequence in bit-level instead of symbol-level.

III. System Model and CoHePNC Procedure

A. System Model

Consider an asymmetric TWRC network, where two source nodes A and B want to exchange information with the help of a relay node R, as A and B are out of each other's transmission range. Each node works in a half-duplex mode equipped with one antenna. Without loss of generality, we consider the channel condition of source-relay link between A and R, L_{ar}, is better than that of L_{br}. Thus, source A uses a higher-order modulation than B. In the following, we mainly consider sources A and B use QPSK and BPSK modulation, respectively, subject to the end-to-end BER requirement as an example. Other higher-modulation CoHePNC can be similarly extended. We assume the symbol-level synchronization at the relay and the channel state information (CSI) is only available at the receivers. The feasibility study for the symbol-level synchronization can be found in [31]. Note that, the carrier-phase synchronization is not assumed in this paper.

The procedure of CoHePNC includes two stages, the multiple access (MA) stage and the broadcast (BC) stage. We focus on the MA stage design, because the main challenges when integrating the channel coding into HePNC in a link-to-link coding reside in the MA stage. To be more precise, the key issues are how to decode the superimposed codewords at the relay to the raw decoding results and how to construct the network-coded sequence, which contains necessary information of the uncoded data in both sources, according to the raw decoding results by the mapping functions. After the MA stage is properly designed, the upgrade of the BC stage from the symbol-level HePNC to CoHePNC is straightforward.

B. CoHePNC Procedure

In this subsection, we present the procedure of QPSK-BPSK CoHePNC with (K, N) channel coding. There are two key design differences between CoHePNC and symbol-level HePNC. The first one is that, in CoHePNC, source A with a higher-order modulation needs to re-organize two N-bit codewords into a new $2N$-bit sequence by intersecting their bits in sequence, and then modulates the $2N$-bit sequence by QPSK. The re-organize process guarantees that the codewords constructed only by the first bit (or the second bit) of the QPSK symbols are valid codewords related to the source channel coding, which is a precondition for the decoding algorithm design at the relay. The second one is that, in CoHePNC, the relay needs to construct a network-coded sequence in the bit-level as discussed in Section IV-D instead of symbol-level in [24]–[30], i.e., the relay needs to construct the network-coded sequence from the decoding results of the superimposed codewords instead of directly from the demodulation results. Also, the network-coded sequence which contains necessary information of the uncoded source data needs to guarantee that each source can recover the other's information finally in the BC stage. We introduce the CoHePNC procedure as follows.

1) Multiple Access Stage: A diagram of the CoHePNC procedure is shown in Fig. 1. We consider that the same (K, N) linear channel coding with the coding efficiency $\frac{K}{N}$ is applied at both sources. Let $\mathbf{u}_{a1} = \{u_{a1}[1], \ldots, u_{a1}[K]\}$ and $\mathbf{u}_{a2} = \{u_{a2}[1], \ldots, u_{a2}[K]\}$ be two uncoded source data at A, and their codewords are $\mathbf{C}_{a1} = \{C_{a1}[1], \ldots, C_{a1}[N]\}$ and $\mathbf{C}_{a2} = \{C_{a2}[1], \ldots, C_{a2}[N]\}$ after encoding. Re-organize $\mathbf{C}_{a1}$ and $\mathbf{C}_{a2}$ to be a $2N$-bit sequence $\mathbf{C}_a = \{C_{a1}[1], C_{a2}[1], \ldots, C_{a1}[N], C_{a2}[N]\}$, i.e., to intersect each bit of $\mathbf{C}_{a1}$ and $\mathbf{C}_{a2}$ in sequence. After that $\mathbf{C}_a$ is modulated by QPSK to be an N-symbol sequence $\mathbf{S}_a = \{S_a[1], \ldots, S_a[N]\}$. For the i-th element in $\mathbf{S}_a$, $S_a[i] = \langle C_{a1}[i], C_{a2}[i] \rangle$, where $\langle , \rangle$ denotes that two bits $C_{a1}[i]$ and $C_{a2}[i]$ are concatenated to be one QPSK symbol $S_a[i]$. At source B, uncoded source data $\mathbf{u}_b = \{u_b[1], \ldots, u_b[K]\}$ is encoded to be $\mathbf{C}_b = \{C_b[1], \ldots, C_b[N]\}$, and then modulated to be an N-

symbol sequence $\mathbf{S}_b = \{S_b[1], \ldots, S_b[N]\}$ by BPSK. Let $\mathcal{M}_m$ be 2^m-QAM/PSK modulation with modulation order m. Let $\mathbf{X}_a$ and $\mathbf{X}_b$ be the transmitted symbols from source A and B, respectively. We have $\mathbf{X}_a = \mathcal{M}_2(\mathbf{S}_a)$ and $\mathbf{X}_b = \mathcal{M}_1(\mathbf{S}_b)$, e.g., with BPSK, the i-th symbol $S_b[i] = 0$ and 1 is mapped to $X_b[i] = 1$ and -1, respectively.

Sources A and B use N symbol durations to transmit $\mathbf{X}_a$ and $\mathbf{X}_b$, respectively. At the i-th symbol duration, one QPSK $X_a[i] = \mathcal{M}_2(S_a[i])$ and one BPSK $X_b[i] = \mathcal{M}_1(S_b[i])$ are transmitted simultaneously and superimposed at the relay. The received signal $Y_r[i]$ at relay R is

$$Y_r[i] = H_a[i]X_a[i] + H_b[i]X_b[i] + N_0, \tag{1}$$

where $H_a[i]$ and $H_b[i]$ are the complex channel gains over links L_{ar} and L_{br}, respectively,[3] and N_0 is the complex Gaussian noise with a variance of $2\sigma^2$. Note that channel gains $H_a[i]$ and $H_b[i]$ are not known by the sources before transmission, and the receivers conduct and obtain the full channel estimations only.

Different from the symbol-level HePNC, where the relay can process the demodulation in each symbol duration, in CoHePNC, the relay needs to obtain the whole codewords $\mathbf{C}_a$ and $\mathbf{C}_b$ in a period of N symbol durations and then processes the decoding with the decoding input $\mathbf{Y}_r = \{Y_r[1], \ldots, Y_r[N]\}$. The final output after the decoding algorithm and mapping process is a well-designed network-coded sequence $\widehat{\mathbf{u}}_r = \{\widehat{u}_r[1], \ldots, \widehat{u}_r[K]\}$, $\widehat{u}_r[i] \in \{00, 01, 11, 10\}$ and $i \in \{1, \ldots, K\}$, where in this paper we use the wide-hat mark $\widehat{}$ to label the estimation results. $\widehat{\mathbf{u}}_r$ contains the necessary information of the uncoded source data $\widehat{\mathbf{u}}_{a1}$, $\widehat{\mathbf{u}}_{a2}$ and $\widehat{\mathbf{u}}_b$ so that each source can obtain the other source's information by recovering $\widehat{\mathbf{u}}_r$ finally in the BC stage. How to construct $\widehat{\mathbf{u}}_r$ is a critical issue. First, the basic requirement is that $\widehat{\mathbf{u}}_r$ contains the necessary information of the uncoded source data. However, $\widehat{\mathbf{u}}_r$ should be constructed with as fewer bits as possible to reduce the transmission load in the BC stage. Also, $\widehat{\mathbf{u}}_r$ should guarantee that the transmission errors happened in the MA stage can be minimized. For 2^{m_a} QAM/PSK-2^{m_b} QAM/PSK CoHePNC, the minimum tuple of $\widehat{u}_r[i]$ is $\min(m_a, m_b)$. For QPSK-BPSK CoHePNC, which implies that $\widehat{u}_r[i] \in \{00, 01, 11, 10\}$, $i \in \{1, \ldots, K\}$. A brief explanation is that $u_r[i]$ at least needs two bits (four-tuple) to contain the information of $u_{a1}[i]$ and $u_{a2}[i]$ even if without considering the impacts of $u_b[i]$. We will show that $\min(m_a, m_b)$ is sufficient in Section IV-D.

One step before obtaining $\widehat{\mathbf{u}}_r$ is to obtain the raw decoding results from the relay decoding algorithm, followed by mapping the raw decoding results to the network-coded sequence $\widehat{\mathbf{u}}_r$ according to mapping function $\mathcal{C}$. We will discuss and compare several possible decoding and mapping solutions in Section V, and then present the proposed full-state sum-product decoding algorithm which utilizes the maximum-state information of $\mathbf{Y}_r$ as the decoding input jointly mapping the raw output of the decoding algorithm with bit-level adaptive mapping functions to obtain the network-coded sequence $\widehat{\mathbf{u}}_r$.

2) Broadcast Stage: Let $\widehat{\mathbf{u}}_r = \langle \widehat{\mathbf{u}}_{r1}, \widehat{\mathbf{u}}_{r2} \rangle$, where $\widehat{\mathbf{u}}_{r1}$ and $\widehat{\mathbf{u}}_{r2}$ denote the bit sequence composed by the first bit and the second bit of $\widehat{u}_r[i]$, respectively. In the BC stage, the relay re-encodes $\widehat{\mathbf{u}}_{r1}$ and $\widehat{\mathbf{u}}_{r2}$ to be N-bit codewords $\mathbf{C}_{r1}$ and $\mathbf{C}_{r2}$, respectively,[4] and then broadcasts the resulting codewords back to the sources. The relay should report which mapping function is selected to the sources in the BC stage. Note that the relay only needs 2 bits to inform which mapping functions is selected, and the overhead depends on how fast the channel changes. Because the bottleneck link L_{br} can only support BPSK subject to the end-to-end BER requirement, the relay uses $2N$ symbol durations to broadcast $\mathbf{C}_{r1}$ and $\mathbf{C}_{r2}$ in sequence in the BC stage. Finally, each source decodes the estimated $\mathbf{C}_{r1}$ and $\mathbf{C}_{r2}$ as $\widehat{\widehat{\mathbf{u}}}_{r1}$ and $\widehat{\widehat{\mathbf{u}}}_{r2}$ by the traditional decoding, respectively, and then obtains each other's information by using the determined mapping function $\mathcal{C}$ and the original information transmitted by themselves. For example, at source A, the estimated i-th bit of $\mathbf{u}_b$ can be obtained by

$$\widehat{\widehat{u}}_b[i] = \underset{u_b[i] \in \{0,1\}}{\operatorname{argmin}} \left| \langle \widehat{\widehat{u}}_{r1}[i], \widehat{\widehat{u}}_{r2}[i] \rangle - \mathcal{C}(\langle u_{a1}[i], u_{a2}[i] \rangle, u_b[i]) \right|^2. \tag{2}$$

Source B can obtain the estimations of $\mathbf{u}_{a1}$ and $\mathbf{u}_{a2}$, denoted as $\widehat{\widehat{\mathbf{u}}}_{a1}$ and $\widehat{\widehat{\mathbf{u}}}_{a1}$, in a similar way.

IV. Design and Optimization Criteria

In this section, repeat-accumulate (RA) coding is studied as an example of the linear channel coding integrated into HePNC. We analyze and compare several relay decoding and mapping solutions, and then elaborate the proposed full-state sum-product decoding algorithm for CoHePNC jointly with the bit-level adaptive mapping function design.

A. Repeat-Accumulate Encoding at Sources

RA coding can be considered as special LDPC codes with low complexity decoding operation, or special Turbo codes with linear complexity encoding operation. We refer the readers to [32]–[34] for more background of the RA codes and the sum-product decoding algorithm.

RA codes with repeat parameter $q = 3$ is applied by both sources A and B. For two uncoded date sequences $\mathbf{u}_{a1} = \{u_{a1}[1], \ldots, u_{a1}[K]\}$ and $\mathbf{u}_{a2} = \{u_{a2}[1], \ldots, u_{a2}[K]\}$ at source A, the codewords are $\mathbf{C}_{a1} = \{C_{a1}[1], \ldots, C_{a1}[N]\}$ and $\mathbf{C}_{a2} = \{C_{a2}[1], \ldots, C_{a2}[N]\}$, respectively. Let $\mathbf{u}'_{a1} = \{u_{a1}[1], u_{a1}[1], u_{a1}[1], \ldots, u_{a1}[K], u_{a1}[K], u_{a1}[K]\}$ be the duplication result of $\mathbf{u}_{a1}$ with duplication parameter $q = 3$. Let $\mathbf{u}''_{a1}$ be the interleaving[5] result of $\mathbf{u}'_{a1}$, and we have $u''_{a1}[i] = u'_{a1}[k]$, $i, k \in \{1, \ldots, N\}$, which denotes that the i-th element in $\mathbf{u}''_{a1}$ equals to the k-th element in $\mathbf{u}'_{a1}$. Similarly, let $\mathbf{u}'_{a2}$, $\mathbf{u}'_b$ and $\mathbf{u}''_{a2}$, $\mathbf{u}''_b$ be the duplication and interleaving results for data flow $\mathbf{u}_{a2}$

[3] We consider both block fading and fast fading channels. In block fading channel, H_a and H_b remain the same during N symbol durations. In fast fading channel, H_a and H_b vary in different symbol durations. In fast fading channel, the mapping function optimization criterion discussed in Section V-B still provides a guideline for how to select a fixed mapping function.

[4] Although theoretically the relay can use any channel coding to re-encode $\widehat{\mathbf{u}}_{r1}$ and $\widehat{\mathbf{u}}_{r2}$, for simplicity, we still consider the relay uses the same channel coding as applied in the source channel coding in the MA stage.

[5] The interleaving pattern is the same and known by all nodes.

and $\mathbf{u}_b$, respectively. For the i-th codeword, $i \in \{2, \ldots, N\}$, we have

$$\begin{aligned} C_{a1}[i] &= C_{a1}[i-1] \oplus u''_{a1}[i] = C_{a1}[i-1] \oplus u'_{a1}[k], \\ C_{a2}[i] &= C_{a2}[i-1] \oplus u''_{a2}[i] = C_{a2}[i-1] \oplus u'_{a2}[k], \\ C_b[i] &= C_b[i-1] \oplus u''_b[i] = C_b[i-1] \oplus u'_b[k], \end{aligned} \tag{3}$$

where $C_{a1}[1] = u''_{a1}[1]$, $C_{a2}[1] = u''_{a2}[1]$ and $C_b[1] = u''_b[1]$, and $\oplus$ stands for the XOR operation.

B. Relay Decoding Solutions Extended From Channel Coded Symmetric PNC

In this subsection, we present and compare the relay decoding and mapping options for channel coded HePNC by extending the decoding and mapping options from the existing channel coded symmetric PNC. For channel coded HePNC, according to whether the codewords $\mathbf{C}_{a1}$, $\mathbf{C}_{a2}$ and $\mathbf{C}_b$ are separately decoded or jointly decoded and how many states the message passing have in the re-designed sum-product decoding algorithm, the solutions for channel coded HePNC at the relay can be summarized as follows.

1) Separately Decoding $\mathbf{C}_{a1}$*,* $\mathbf{C}_{a2}$ *and* $\mathbf{C}_b$*:* A straightforward solution extended from the symmetric channel coded PNC is to perform three traditional sum-product decoding processes to decode each of $\mathbf{C}_{a1}$, $\mathbf{C}_{a2}$ and $\mathbf{C}_b$ individually, and then obtain the network-coded sequence $\widehat{\mathbf{u}}_r = \langle \widehat{\mathbf{u}}_{r1}, \widehat{\mathbf{u}}_{r2} \rangle$ by letting $\widehat{\mathbf{u}}_{r1} = \widehat{\mathbf{C}}_{a1}$ XOR $\widehat{\mathbf{C}}_b$ and $\widehat{\mathbf{u}}_{r2} = \widehat{\mathbf{C}}_{a2}$ XOR $\widehat{\mathbf{C}}_b$. In this method, the mapping process is included by the XOR operation obtaining $\widehat{\mathbf{u}}_{r1}$ and $\widehat{\mathbf{u}}_{r2}$. This method is not optimal due to over-decoding [13], [35], as the relay only needs to obtain the network-coded forms $\mathbf{u}_{r1}$ and $\mathbf{u}_{r2}$ instead of obtaining $\widehat{\mathbf{C}}_{a1}$, $\widehat{\mathbf{C}}_{a2}$ and $\widehat{\mathbf{C}}_b$ explicitly.

2) Separately Decoding $\mathbf{C}_{a1}$ *XOR* $\mathbf{C}_b$ *and* $\mathbf{C}_{a2}$ *XOR* $\mathbf{C}_b$*:* By extending the decoding solutions for symmetric BPSK-BPSK channel coded PNC [12], we can decompose the QPSK-BPSK channel coded HePNC into two BPSK-BPSK channel coded PNC and perform two BPSK-BPSK symmetric channel coded PNC decoding individually. In other words, it is to consider codewords $\mathbf{C}_{a1}$ and $\mathbf{C}_b$, and $\mathbf{C}_{a2}$ and $\mathbf{C}_b$ as separate flows with the solution of BPSK-BPSK channel coded PNC for each flow. We use one flow $\mathbf{C}_{a1}$ and $\mathbf{C}_b$ to explain, and the solution to the other flow is equivalent. For BPSK-BPSK channel coded PNC, when sources apply the same linear channel coding, the result of $\mathbf{C}_{a1}$ XOR $\mathbf{C}_b$ is still a valid codeword associated with the channel coding applied at sources [12]. To apply this property in the sum-product decoding algorithm, the i-th input of the evidence node, $i \in \{1, \ldots, N\}$ can be a two-state message $\Pr\{(\widehat{C}_{a1}[i], \widehat{C}_b[i]) = (0,0)\} + \Pr\{(\widehat{C}_{a1}[i], \widehat{C}_b[i]) = (1,1)\}$ and $\Pr\{(\widehat{C}_{a1}[i], \widehat{C}_b[i]) = (0,1)\} + \Pr\{(\widehat{C}_{a1}[i], \widehat{C}_b[i]) = (1,0)\}$, i.e., the binary results of $\widehat{\mathbf{C}}_{a1}$ XOR $\widehat{\mathbf{C}}_b$. Thus, the traditional sum-product decoding algorithm can be directly applied.

It was found that for BPSK-BPSK channel coded PNC, the input of the sum-product decoding algorithm at the relay can be a three-state message [13], [18] instead of a two-state one, i.e., $\Pr\{(\widehat{C}_{a1}[i], \widehat{C}_b[i]) = (0,0)\}$, $\Pr\{(\widehat{C}_{a1}[i], \widehat{C}_b[i]) = (0,1)\}$ $+ \Pr\{(\widehat{C}_{a1}[i], \widehat{C}_b[i]) = (1,0)\}$ and $\Pr\{(\widehat{C}_{a1}[i], \widehat{C}_b[i]) = (1,1)\}$. However, it brings new challenges that the traditional sum-product decoding algorithm needs to be re-designed to fit the PNC feature. The authors in [14], [15] further generalized [13], [18] and proposed a four-state message sum-product decoding algorithm, where the i-th input of the decoding algorithm at the relay are four-state message $\Pr\{(\widehat{C}_{a1}[i], \widehat{C}_b[i]) = (0,0)\}$, $\Pr\{(\widehat{C}_{a1}[i], \widehat{C}_b[i]) = (0,1)\}$, $\Pr\{(\widehat{C}_{a1}[i], \widehat{C}_b[i]) = (1,0)\}$ and $\Pr\{(\widehat{C}_{a1}[i], \widehat{C}_b[i]) = (1,1)\}$ and showed that the four-state sum-product decoding algorithm outperforms the two-state and three-state decoding algorithms.

3) Jointly Decoding $\mathbf{C}_{a1}$*,* $\mathbf{C}_{a2}$ *and* $\mathbf{C}_b$*:* The decoding solutions [12]–[15], [18] focused on channel coded PNC design under symmetric TWRC, where BPSK modulation and the same linear channel coding are applied at both sources. The authors in [22], [23] studied symmetric channel coded PNC with QPSK/PAM modulations with XOR mapping. An upgrade from [22], [23] for QPSK-BPSK channel coded HePNC is to pass the message with four-state results of $\mathbf{C}_{a1}$ XOR $\mathbf{C}_b$ and $\mathbf{C}_{a2}$ XOR $\mathbf{C}_b$, i.e.,

$$\begin{aligned} &\Pr\{(\widehat{C}_{a1}[i], \widehat{C}_{a2}[i], \widehat{C}_b[i]) = (0,0,0) \cup (1,1,1)\}, \\ &\Pr\{(\widehat{C}_{a1}[i], \widehat{C}_{a2}[i], C_b[i]) = (0,1,0) \cup (1,0,1)\}, \\ &\Pr\{(\widehat{C}_{a1}[i], \widehat{C}_{a2}[i], \widehat{C}_b[i]) = (1,1,0) \cup (0,0,1)\}, \\ &\Pr\{(\widehat{C}_{a1}[i], \widehat{C}_{a2}[i], \widehat{C}_b[i]) = (1,0,0) \cup (0,1,1)\}. \end{aligned}$$

Followed by using the four-state message decoding algorithm in [14], [15] with the above four-state message as the decoding input.

For higher-order modulation HePNC, e.g., QPSK-BPSK channel coded HePNC, $\mathbf{C}_{a1}$ and $\mathbf{C}_{a2}$ can be jointly decoded together with $\mathbf{C}_b$. In this paper, we propose a full-state sum-product decoding algorithm for QPSK-BPSK CoHePNC under the asymmetric TWRC scenario jointly with a bit-level adaptive mapping function design. The new contributions of the decoding algorithm proposed in this paper compared with the existing work include two parts: first, we design the message updating rules for QPSK-BPSK CoHePNC with full-state message passing, which are different from the updating rules of the existing symmetric channel coded PNC; second, we further prove that bit-level adaptive mapping design should be applied to obtain the network-coded sequence instead of symbol-level mapping. The proposed adaptive mapping design can also be applied to optimize the symmetric channel coded PNC under symmetric TWRC scenario.

C. Full-State Sum-Product Decoding Algorithm

In this subsection, we elaborate the proposed full-state decoding algorithm at the relay. The first step is to obtain the raw eight-ary estimation results of $\widehat{\mathbf{u}}_{a1}$, $\widehat{\mathbf{u}}_{a2}$ and $\widehat{\mathbf{u}}_b$ from the received superimposed signals $\mathbf{Y}_r$. For the QPSK-BPSK link-to-link channel coded HePNC, the maximum state at the relay is eight. Thus, in the following, we may use eight-state and full-state interchangeably. The second step, which will be discussed in Section IV-D, is to obtain the four-ary network-coded sequence $\widehat{\mathbf{u}}_r$ from the raw eight-ary decoding results.

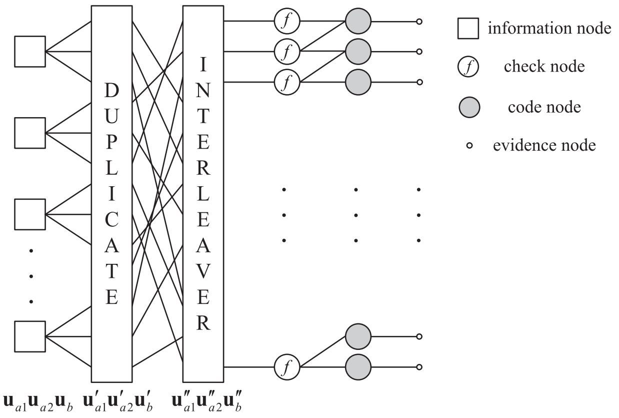
D U P L I C A T E
I N T E R L E A V E R
f
information node
check node
code node
evidence node
$\mathbf{u}_{a1}\mathbf{u}_{a2}\mathbf{u}_b$
$\mathbf{u}'_{a1}\mathbf{u}'_{a2}\mathbf{u}'_b$
$\mathbf{u}''_{a1}\mathbf{u}''_{a2}\mathbf{u}''_b$

Fig. 2. Tanner graph.

As the same interleaver is applied by both sources, we can virtually combine the uncoded data sequences $\mathbf{u}_{a1}, \mathbf{u}_{a2}$ and $\mathbf{u}_b$ as an ensemble $\mathbf{u}_{a1}\mathbf{u}_{a2}\mathbf{u}_b$ for concise writing, where the i-th element $u_{a1}[i]u_{a2}[i]u_b[i] \in \{000, 001, 010, 011, 110, 111, 100, 101\}$, $i \in \{1, \ldots, K\}$. Equivalently, we can obtain the duplication result $\mathbf{u}'_{a1}\mathbf{u}'_{a1}\mathbf{u}'_b$, interleaving result $\mathbf{u}''_{a1}\mathbf{u}''_{a1}\mathbf{u}''_b$ and codeword $\mathbf{C}_{a1}\mathbf{C}_{a2}\mathbf{C}_b$, where $u'_{a1}[i]u'_{a2}[i]u'_b[i] = u''_{a1}[k]u''_{a2}[k]u''_b[k]$ and $i, k \in \{1, \ldots, N\}$. The corresponding Tanner graph [34] is shown in Fig. 2. The square nodes denote the information nodes, where the i-th information node stores $\Pr\{\widehat{u}_{a1}[i]\widehat{u}_{a2}[i]\widehat{u}_b[i]\}$, $i \in \{1, \ldots, K\}$. The blocks of duplicate and interleaver store the probabilities of $\widehat{\mathbf{u}}'_{a1}\widehat{\mathbf{u}}'_{a2}\widehat{\mathbf{u}}'_b$ and $\widehat{\mathbf{u}}''_{a1}\widehat{\mathbf{u}}''_{a2}\widehat{\mathbf{u}}''_b$, respectively. The round nodes with function $f(.)$ are the check nodes, which denote that the edges connected to the same check nodes need to satisfy the constraint $f(.)$. The dark circles are the code nodes, which store the probabilities of $\widehat{\mathbf{C}}_{a1}\widehat{\mathbf{C}}_{a2}\widehat{\mathbf{C}}_b$. The small circles are the evidence nodes, which denote the input of the decoding algorithm.

The encoding process can be considered as reading the Tanner graph as shown in Fig. 2 from the left to the right. The decoding process starts from adding input into the evidence nodes on the rightmost and then passes the eight-state message iteratively between the information nodes and code nodes. The message are the probabilities of $\Pr\{\widehat{C}_{a1}[i]\widehat{C}_{a2}[i]\widehat{C}_b[i]\}$, $\Pr\{\widehat{u}'_{a1}[i]\widehat{u}'_{a2}[i]\widehat{u}'_b[i]\}$, $\Pr\{\widehat{u}''_{a1}[i]\widehat{u}''_{a2}[i]\widehat{u}''_b[i]\}$ and $\Pr\{\widehat{u}_{a1}[i]\widehat{u}_{a2}[i]\widehat{u}_b[i]\}$ depending on the type of nodes that the messages are associated with. We present the decoding algorithm of CoHePNC as follows, where steps 1) and 2) are the decoding settings, and steps 3) and 4) are the iteration bodies. Step 5) denotes the termination condition.

1) Initialization: Let $\mathbf{P} = (p_1, p_2, p_3, p_4, p_5, p_6, p_7, p_8)$ and $\mathbf{Q} = (q_1, q_2, q_3, q_4, q_5, q_6, q_7, q_8)$ be the message input from two different nodes. All the messages associated with the edges are set to be $(\frac{1}{8}, \frac{1}{8}, \frac{1}{8}, \frac{1}{8}, \frac{1}{8}, \frac{1}{8}, \frac{1}{8}, \frac{1}{8})$ initially except for the messages on the edges connected to the evidence nodes.

2) Input of the Evidence Nodes: The input of the decoding algorithm is the message from the evidence nodes, which contains the eight-state probabilities of $\widehat{\mathbf{C}}_{a1}\widehat{\mathbf{C}}_{a2}\widehat{\mathbf{C}}_b$ obtained from the superimposed signals $\mathbf{Y}_r$ in (1). Denote the input of the i-th evidence node as

$$p_{input}[i] = (p_1, p_2, p_3, p_4, p_5, p_6, p_7, p_8). \tag{4}$$

Define function $g(.)$ as

$$g(x_a, x_b) = \frac{1}{\beta} \exp\left(\frac{-|Y_k[i] - H_a x_a - H_b x_b|^2}{2\sigma^2} \right). \tag{5}$$

We specify $p_1 = g(\frac{\sqrt{2}+\sqrt{2}j}{2}, 1)$, $p_2 = g(\frac{\sqrt{2}+\sqrt{2}j}{2}, -1)$, $p_3 = g(\frac{-\sqrt{2}+\sqrt{2}j}{2}, 1)$, $p_4 = g(\frac{-\sqrt{2}+\sqrt{2}j}{2}, -1)$, $p_5 = g(\frac{-\sqrt{2}-\sqrt{2}j}{2}, 1)$, $p_6 = g(\frac{-\sqrt{2}-\sqrt{2}j}{2}, -1)$, $p_7 = g(\frac{\sqrt{2}-\sqrt{2}j}{2}, 1)$ and $p_8 = g(\frac{\sqrt{2}-\sqrt{2}j}{2}, -1)$, where j is the imaginary part and β is a normalization parameter to satisfy that $\sum_{i=1}^{8} p_i = 1$. We can find that $p_i, i \in \{1, \ldots, 8\}$ in $p_{input}[i]$ denotes one of the probabilities of $X_a[i] \in \{\frac{\sqrt{2}+\sqrt{2}j}{2}, \frac{-\sqrt{2}+\sqrt{2}j}{2}, \frac{-\sqrt{2}-\sqrt{2}j}{2}, \frac{\sqrt{2}-\sqrt{2}j}{2}\}$ and $X_b[i] \in \{1, -1\}$.

3) Message Updating for the Variable Nodes: Both code nodes and information nodes are variable nodes. Each variable node is connected to three other nodes (except for the code node at the bottom). Denote the output message of the variable node as $\mathrm{VAR}(\mathbf{P}, \mathbf{Q})$, where $\mathbf{P}$ and $\mathbf{Q}$ denote the message input from two connected edges and the output is the updated message on the rest edge. From [13], [18], we can obtain that the output message for the variable node is

$$\mathrm{VAR}(\mathbf{P}, \mathbf{Q}) = \frac{(p_1 q_1, p_2 q_2, p_3 q_3, p_4 q_4, p_5 q_5, p_6 q_6, p_7 q_7, p_8 q_8)}{\alpha}, \tag{6}$$

where α is a normalization parameter which satisfies that $\sum_{i=1}^{8} \frac{1}{\alpha} p_i q_i = 1$.

4) Message Updating for the Check Nodes: One of the key issues in the sum-product decoding algorithm applied in PNC is how to design the message updating rules for check nodes. Each check node is connected to three edges (except for the check node at the top). Denote the output message of the check node as $\mathrm{CHK}(\mathbf{P}, \mathbf{Q})$, where $\mathbf{P}$ and $\mathbf{Q}$ denote the message input from two connected edges and the output is the updated message on the rest edge. As Gray mapping is applied at source A, i.e., $\langle \mathbf{C}_{a1}, \mathbf{C}_{a2} \rangle \in \{00, 01, 11, 10\}$ are modulated to be $\mathbf{X}_a \in \{\frac{\sqrt{2}+\sqrt{2}j}{2}, \frac{-\sqrt{2}+\sqrt{2}j}{2}, \frac{-\sqrt{2}-\sqrt{2}j}{2}, \frac{\sqrt{2}-\sqrt{2}j}{2}\}$ on the constellation map, respectively, for the i-th symbol duration, re-write (1) as

$$Y_r[i] = H_a[i] \left\{ \frac{\sqrt{2}}{2} j\big(1 - 2C_{a1}[i]\big) + \frac{\sqrt{2}}{2}\big(1 - 2C_{a2}[i]\big) \right\} + H_b[i](1 - 2C_b[i]) + N_0, \tag{7}$$

where $C_{a1}[i], C_{a2}[i], C_b[i] \in \{0, 1\}$. From (3) and (7), we have $C_{a1}[i] = C_{a1}[i-1] \oplus u'_{a1}[k]$, $C_{a2}[i] = C_{a2}[i-1] \oplus u'_{a2}[k]$ and $C_b[i] = C_b[i-1] \oplus u'_b[k]$. Note that, we have substituted $u''_{a1}[i]u''_{a2}[i]u''_b[i]$ with $u'_{a1}[k]u'_{a2}[k]u'_b[k]$.

Consider the case that two input messages $\mathbf{P}$ and $\mathbf{Q}$ defined in (6) are from the code nodes and the output is to the edge connected to the interleaver. To obtain the function $f(.)$ processed in the check node, we are targeting at obtaining

$$\Pr\{\widehat{u}'_{a1}[k]\widehat{u}'_{a2}[k]\widehat{u}'_{b}[k]\} =$$
$$f(\Pr\{\widehat{C}_{a1}[i]\widehat{C}_{a2}[i]\widehat{C}_{b}[i]\}, \Pr\{\widehat{C}_{a1}[i-1]\widehat{C}_{a2}[i-1]\widehat{C}_{b}[i-1]\}). \tag{8}$$

From (8), we have

$$\begin{aligned}&\Pr\big(\widehat{u}'_{a1}[k]\widehat{u}'_{a2}[k]\widehat{u}'_{b}[k] = 000|\mathbf{P},\mathbf{Q}\big)\\ &= \sum_{i=1}^{8} \Pr\big(\widehat{C}_{a1}[i]\widehat{C}_{a2}[i]\widehat{C}_{b}[i] = \widehat{C}_{a1}[i-1]\widehat{C}_{a2}[i-1]\widehat{C}_{b}[i-1]\big)\\ &= \sum_{i=1}^{8} p_i q_i \triangleq \lambda_1.\end{aligned} \tag{9}$$

Similar to (9), we have

$$\begin{bmatrix}\lambda_2\\ \lambda_3\\ \lambda_4\\ \lambda_5\\ \lambda_6\\ \lambda_7\\ \lambda_8\end{bmatrix} \triangleq \begin{bmatrix}\Pr(\widehat{u}'_{a1}[k]\widehat{u}'_{a2}[k]\widehat{u}'_{b}[k] = 001|\mathbf{P},\mathbf{Q})\\ \Pr(\widehat{u}'_{a1}[k]\widehat{u}'_{a2}[k]\widehat{u}'_{b}[k] = 010|\mathbf{P},\mathbf{Q})\\ \Pr(\widehat{u}'_{a1}[k]\widehat{u}'_{a2}[k]\widehat{u}'_{b}[k] = 011|\mathbf{P},\mathbf{Q})\\ \Pr(\widehat{u}'_{a1}[k]\widehat{u}'_{a2}[k]\widehat{u}'_{b}[k] = 110|\mathbf{P},\mathbf{Q})\\ \Pr(\widehat{u}'_{a1}[k]\widehat{u}'_{a2}[k]\widehat{u}'_{b}[k] = 111|\mathbf{P},\mathbf{Q})\\ \Pr(\widehat{u}'_{a1}[k]\widehat{u}'_{a2}[k]\widehat{u}'_{b}[k] = 100|\mathbf{P},\mathbf{Q})\\ \Pr(\widehat{u}'_{a1}[k]\widehat{u}'_{a2}[k]\widehat{u}'_{b}[k] = 101|\mathbf{P},\mathbf{Q})\end{bmatrix}$$
$$= \begin{bmatrix} q_2\, q_1\, q_4\, q_3\, q_6\, q_5\, q_8\, q_7\\ q_3\, q_4\, q_1\, q_2\, q_7\, q_8\, q_5\, q_6\\ q_4\, q_3\, q_2\, q_1\, q_8\, q_7\, q_6\, q_5\\ q_5\, q_6\, q_7\, q_8\, q_1\, q_2\, q_3\, q_4\\ q_6\, q_5\, q_8\, q_7\, q_2\, q_1\, q_4\, q_3\\ q_7\, q_8\, q_5\, q_6\, q_3\, q_4\, q_1\, q_2\\ q_8\, q_7\, q_6\, q_5\, q_4\, q_3\, q_2\, q_1\end{bmatrix} \begin{bmatrix}p_1\\ p_2\\ p_3\\ p_4\\ p_5\\ p_6\\ p_7\\ p_8\end{bmatrix} \tag{10}$$

Thus, the function $f(.)$ at the check node for the case that the input message are from two code nodes is summarized in (9) and (10). Another two cases are that the input message are from $\widehat{u}'_{a1}[k]\widehat{u}'_{a2}[k]\widehat{u}'_{b}[k]$ $(u''_{a1}[i]u''_{a2}[i]u''_{b}[i])$ and $\widehat{C}_{a1}[i]\widehat{C}_{a2}[i]\widehat{C}_{b}[i]$ or from $\widehat{u}'_{a1}[k]\widehat{u}'_{a2}[k]\widehat{u}'_{b}[k]$ $(u''_{a1}[i]u''_{a2}[i]u''_{b}[i])$ and $\widehat{C}_{a1}[i-1]\widehat{C}_{a2}[i-1]\widehat{C}_{b}[i-1]$, and the corresponding output are $\widehat{C}_{a1}[i-1]\widehat{C}_{a2}[i-1]\widehat{C}_{b}[i-1]$ and $\widehat{C}_{a1}[i]\widehat{C}_{a2}[i]\widehat{C}_{b}[i]$, respectively. For these two cases, The same updating rules as shown in (9) and (10) can be similarly obtained. Thus, the updating rules for the check nodes can be summarized as

$$\mathrm{CHK}(\mathbf{P},\mathbf{Q}) = (\lambda_1,\lambda_2,\lambda_3,\lambda_4,\lambda_5,\lambda_6,\lambda_7,\lambda_8). \tag{11}$$

5) Iteration Termination: The message is passed iteratively between the code nodes and the information nodes with the updating rules summarized in (6) and (11) starting from the input of the evidence nodes summarized in (4) and (5). By setting a proper iteration termination rounds, either by setting iteration rounds or BER requirement, the output of the i-th information node is

$$p_{\text{output}}[i] = \mathrm{VAR}(\mathrm{VAR}(\mathbf{P}_1,\mathbf{P}_2),\mathbf{P}_3), \tag{12}$$

where $\mathbf{P}_1$, $\mathbf{P}_2$ and $\mathbf{P}_3$ denote for the input message on the three edges connected to the i-th information node. Thus, raw decoding result $\widehat{u}_{a1}[i]\widehat{u}_{a2}[i]\widehat{u}_{b}[i]$ can be obtain by selecting the maximum probabilities in $p_{\text{output}}[i]$.

D. Bit-level Mapping Function Design

Although the estimations of the uncoded source data is $2^{m_a+m_b}$-ary, the relay only needs to construct a $2^{\max(m_a,m_b)}$-ary network-coded sequence benefiting from the network coding. Each source can recover the other's information after obtaining the network-coded sequence by the help of the mapping function $\mathcal{C}$ and the original information transmitted by itself as (2). In this subsection, we discuss how to map the $2^{m_a+m_b}$-ary raw decoding result $\widehat{\mathbf{u}}_{a1}\widehat{\mathbf{u}}_{a2}\widehat{\mathbf{u}}_{b}$ to the $2^{\max\{m_a,m_b\}}$-ary network-coded sequence $\widehat{\mathbf{u}}_r$. With the traditional XOR mapping [12]–[14], [18], the i-th symbol $\widehat{u}_r[i]$ can be obtained by $\widehat{u}_r[i] = \langle \widehat{u}_{r1}[i], \widehat{u}_{r2}[i]\rangle = \langle \widehat{u}_{a1}[i]\oplus\widehat{u}_b[i], \widehat{u}_{a2}[i]\oplus\widehat{u}_b[i]\rangle$. In the following, we show that the traditional XOR mapping is not optimal, and bit-level adaptive mapping functions should be designed and applied according to the source-relay channel conditions. Note that, the bit-level mapping function design proposed in CoHePNC is different from the symbol-level mapping function design in symbol-level HePNC [24]–[30]. In the symbol-level HePNC, the relay tries to map the demodulation results $\widehat{\mathbf{C}}_{a1}\widehat{\mathbf{C}}_{a2}\widehat{\mathbf{C}}_{b}$ directly to the network-coded symbols $\widehat{\mathbf{u}}_r$. However, in CoHePNC, $\widehat{\mathbf{C}}_{a1}\widehat{\mathbf{C}}_{a2}\widehat{\mathbf{C}}_{b}$ are first decoded to be $\widehat{\mathbf{u}}_{a1}\widehat{\mathbf{u}}_{a2}\widehat{\mathbf{u}}_{b}$, and then the network-coded sequence is obtained from mapping $\widehat{\mathbf{u}}_{a1}\widehat{\mathbf{u}}_{a2}\widehat{\mathbf{u}}_{b}$ to $\widehat{\mathbf{u}}_r$. Thus, the bit-level mapping function design needs to consider the impact of the proposed decoding algorithm.

We use an example to show why the adaptive bit-level mapping design is necessary. Define γ and θ as the amplitude ratio and the phase shift difference of the two source-relay channels, we have $H_a = H_b\gamma\exp(j\theta)$. Consider the received constellation map at the relay in the i-th symbol duration as shown in Fig. 3(a), where $\gamma = |\frac{H_b}{H_a}| \approx \frac{\sqrt{2}}{2}$ and phase shift $\theta = 0$. The Euclidean distance between constellation points $C_{a1}[i]C_{a2}[i]C_b[i] = 000$ and 001 is small, so is that between 110 and 101. Assume that the correct $C_{a1}[i]C_{a2}[i]C_b[i] = 010$. If without noise, the input of the i-th evidence node $p_{input}[i] = (0, 0, 1, 0, 0, 0, 0, 0, 0)$, i.e., $\Pr\{C_{a1}[i]C_{a2}[i]C_b[i] = 010\} = 1$. However, with noise, due to the small Euclidean distance between constellation points 010 and 001, there is an error probability that $\Pr\{\widehat{C}_{a1}[i]\widehat{C}_{a2}[i]\widehat{C}_{b}[i] = 001\}$ is the largest instead of $\Pr\{\widehat{C}_{a1}[i]\widehat{C}_{a2}[i]\widehat{C}_{b}[i] = 010\}$, i.e., the input of the i-th evidence node implies that the codeword $C_{a1}[i]C_a[i]C_b[i]$ is 001 in error instead of 010. This error probability increases when the Euclidean distance between 010 and 001 decreases. Note that when two different constellation points perfectly superimposed, which is known as the singular fade states (SFS) [27].

We analyze the impact that for the input of the i-th evidence code, $\Pr\{\widehat{C}_{a1}[i]\widehat{C}_{a2}[i]\widehat{C}_{b}[i] = 001\}$ has the largest probability in error instead of $\Pr\{\widehat{C}_{a1}[i]\widehat{C}_{a2}[i]\widehat{C}_{b}[i] = 010\}$. For simplicity, we consider that the input of the i-th evidence node is 001 instead of 010 to stand for that $\Pr\{\widehat{C}_{a1}[i]\widehat{C}_{a2}[i]\widehat{C}_{b}[i] = 001\}$ has the largest probability. During each round of iteration, to update the i-th check node, the two input messages $\Pr\{\widehat{C}_{a1}[i-1]\widehat{C}_{a2}[i-1]\widehat{C}_{b}[i-1]\}$ and $\Pr\{\widehat{C}_{a1}[i]\widehat{C}_{a2}[i]\widehat{C}_{b}[i]\}$ are from the i-th code

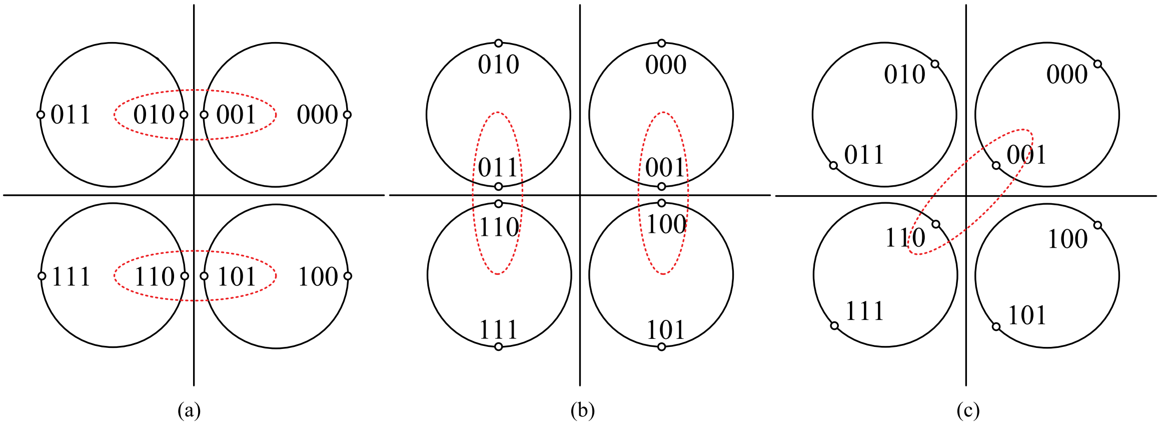

Fig. 3. Constellation maps with difference phase shift θ. (a) $\theta = 0$. (b) $\theta = \frac{\pi}{2}$. (c) $\theta = \frac{\pi}{4}$.

TABLE I
CONSTRAINTS BETWEEN $C_{a1}[i]C_{a2}[i]C_b[i]$, $C_{a1}[i-1]C_{a2}[i-1]C_b[i-1]$ AND $u''_{a1}[i]u''_{a2}[i]u''_b[i]$

$C_{a1}[i-1]C_{a2}[i-1]C_b[i-1]$	000	001	010	011	110	111	100	101
$\widehat{u}''_{a1}[i]\widehat{u}''_{a2}[i]\widehat{u}''_b[i]$ when $C_{a1}[i]C_{a2}[i]C_b[i] = 001$	001	000	011	010	111	110	101	100
$\widehat{u}''_{a1}[i]\widehat{u}''_{a2}[i]\widehat{u}''_b[i]$ when $C_{a1}[i]C_{a2}[i]C_b[i] = 010$	010	011	000	001	100	101	110	111

node and the $(i-1)$-th code node, respectively. As $C_{a1}[i-1]C_{a2}[i-1]C_b[i-1]$ and $C_{a1}[i]C_{a2}[i]C_b[i]$ are independent [13], the output of the i-th code node $u''_{a1}[i]u''_{a2}[i]u''_b[i]$ is summarized in Table I according to (11), where $\widehat{C}_{a1}[i]\widehat{C}_{a2}[i]\widehat{C}_b[i]$ equals 011 falsely or 010 correctly and $\widehat{C}_{a1}[i-1]\widehat{C}_{a2}[i-1]\widehat{C}_b[i-1]$ equals $\{000, 001, 010, 011, 110, 111, 100, 101\}$ with the same probability $\frac{1}{8}$. The estimation $\widehat{u}''_{a1}[i]\widehat{u}''_{a2}[i]\widehat{u}''_b[i]$ directly impacts on the estimation of $\widehat{u}_{a1}[k]\widehat{u}_{a2}[k]\widehat{u}_b[k]$, as $u''_{a1}[i]u''_{a2}[i]u''_b[i] = u'_{a1}[k]u'_{a2}[k]u'_b[k]$, and $u'_{a1}[k]u'_{a2}[k]u'_b[k]$ is the duplication of $u_{a1}[\lceil\frac{k}{3}\rceil]u_{a2}[\lceil\frac{k}{3}\rceil]u_b[\lceil\frac{k}{3}\rceil]$. According to Table I, there is a larger error probability that $\widehat{u}''_{a1}[i]\widehat{u}''_{a2}[i]\widehat{u}''_b[i]$ is estimated to be $\{001, 000, 011, 010, 111, 110, 101, 100\}$ falsely instead of $\{010, 011, 000, 001, 100, 101, 110, 111\}$ correctly. Thus, to minimize the estimation error in the uncoded source data $u_{a1}[\lceil\frac{k}{3}\rceil]u_{a2}[\lceil\frac{k}{3}\rceil]u_b[\lceil\frac{k}{3}\rceil]$, each column of Table I should be mapped to the same $\widehat{u}_r[i]$. In this way, even $\widehat{u}''_{a1}[i]\widehat{u}''_{a2}[i]\widehat{u}''_b[i]$ is falsely estimated, the resulting $\widehat{u}_r[i]$ is still correct. Thus, for the case of Fig. 3(a), after obtaining $p_{output}[i]$ in (12), we can obtain the network-coded sequence $\widehat{u}_r[i]$ by the following mapping function

$$\widehat{u}_r[i] = \begin{cases} 00 & \text{when } \widehat{u}_{a1}[i]\widehat{u}_{a2}[i]\widehat{u}_b[i] = 000 \text{ and } 011, \\ 01 & \text{when } \widehat{u}_{a1}[i]\widehat{u}_{a2}[i]\widehat{u}_b[i] = 010 \text{ and } 001, \\ 11 & \text{when } \widehat{u}_{a1}[i]\widehat{u}_{a2}[i]\widehat{u}_b[i] = 110 \text{ and } 101, \\ 10 & \text{when } \widehat{u}_{a1}[i]\widehat{u}_{a2}[i]\widehat{u}_b[i] = 100 \text{ and } 111. \end{cases} \quad (13)$$

The above analysis shows that by properly designing the bit-level mapping function to map the eight-ary $\widehat{\mathbf{u}}_{a1}\widehat{\mathbf{u}}_{a1}\widehat{\mathbf{u}}_b$ to four-ary $\widehat{\mathbf{u}}_r$, we try to minimize the decoding errors caused from the smallest Euclidean distance between different constellation points. The mapping function summarized in (13) is the mapping function $\mathcal{C}_1$ summarized in Table II. Another two cases of the smallest Euclidean distance are shown in Fig. 3(b) and (c), respectively, and mapping functions $\mathcal{C}_2$ and $\mathcal{C}_3$ can be obtained similar to the analysis to Fig. 3(a). Note that there are other ones available besides the three mapping functions listed in Table II. However, when $\gamma \in (0, 1)$ and $\theta \in (0, 2\pi)$, the three mapping functions listed are optimal in different regions as shown in Fig. 4 obtained by exhaustive search, where the smallest Euclidean distance between different constellation points are maximized. Given two source-relay channel conditions, i.e., given parameters γ and θ, where γ and θ are the received amplitude ratio and the phase shift difference, the relay can adaptively select the mapping functions according to the source-relay channel conditions γ and θ, and then obtain the mapping function $\mathcal{C}$ by looking up Table II. In Table II, the horizontal bits are the symbols from source A, and the vertical bits are the symbols from source B, and $\mathcal{C}_1$, $\mathcal{C}_2$ and $\mathcal{C}_3$ are the bit-level mapping functions labelled in Fig. 4.

TABLE II
MAPPING FUNCTIONS

	00	01	11	10
0	00	01	11	10
1($\mathcal{C}_1$)	01	00	10	11
1($\mathcal{C}_2$)	10	11	01	00
1($\mathcal{C}_3$)	11	10	00	01

V. PERFORMANCE EVALUATION

In this section, the performance CoHePNC under asymmetric TWRC scenario is studied. The existing solutions extended from the symmetric channel coded PNC are compared with

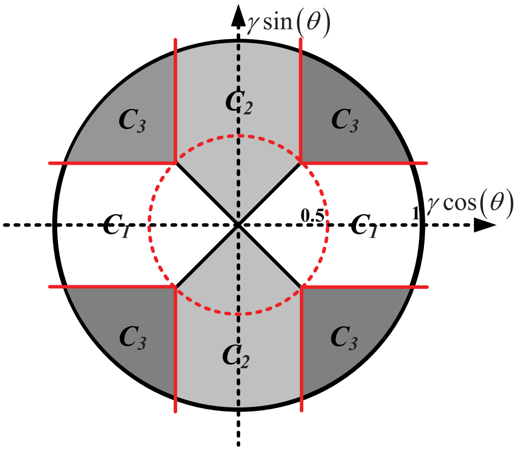

Fig. 4. Bit-level adaptive mapping functions.

the proposed CoHePNC under Gaussian and Rayleigh fading channels. RA codes with duplication $q = 3$ are applied by both sources with a codeword length of 4096 bits. We let all the nodes transmit signals with the same symbol energy E_s and set the average received SNR of all links be proportional to $d^{-\alpha}$, where d is the link distance and the path loss exponent $\alpha = 3$. The phase shift difference θ between the superimposed signals is uniformly distributed between $[0, 2\pi)$.

A. Comparisons of Several Decoding Solutions

In this subsection, we compare the solutions extended from the symmetric PNC with the proposed CoHePNC in terms of relay error rate (RER) as introduced in Section IV-B under Gaussian channels. Separate-two-state denotes the upgrade from [12], separate-four-state denotes the upgrades from [14], [15], [23], joint-four-state and XorHePNC denote the upgrade from [22], [23] with four-state or eight-state passing message with XOR mapping, and CoHePNC denotes the proposed decoding algorithm. Throughout this paper, SNR is defined as the received SNR with the unit of dB. For Gaussian channels, SNR can be calculated as $\text{SNR(dB)} = 10\log_{10}\frac{E_r}{N_0}$, where E_r denotes the received symbol energy, and N_0 is the noise spectral density. For Rayleigh fading channels, SNR denotes the average received SNR. RER is defined as $\text{RER} = \frac{\Pr\{\widehat{\mathbf{u}}_{r1} \neq \mathbf{u}_{r1}\} + \Pr\{\widehat{\mathbf{u}}_{r2} \neq \mathbf{u}_{r2}\}}{2}$. Note that in Fig. 5 we only compare the error performance of the MA stage for these decoding algorithms as they share the same BC stage. Thus, a worse error performance in the MA stage directly affects the overall end-to-end BER performance.

In Fig. 5, the error performance RER improves with either a larger SNR_{ar} or SNR_{br}. For a fair comparison, we fixed $\text{SNR}_{br} = -1.5$ dB and gradually increase SNR_{ar} from 0 dB to 10 dB. We can observe that comparing separate-two-state and separate-four-state, increasing the state of the passing message improves the RER performance with an increase of calculation complexity at the relay. Joint-four-state outperforms the separate decoding ones, because the full channel received information can be applied without being processed before the input of the decoding algorithm. In the three jointly decoding algorithms, increasing the state of the passing message from four to eight greatly improves the relay error performance. We further compare the two joint-eight-state algorithms, which both apply the full-state decoding with difference of mapping function design. It shows that bit-level adaptive mapping function design can further improve the RER performance with 1 dB gain as the fixed XOR mapping function design may suffer from the SFS effects resulting in a higher error rate. The adaptive mapping design tries to minimize RER by selecting the proper mapping functions according to the two source-relay channel conditions.

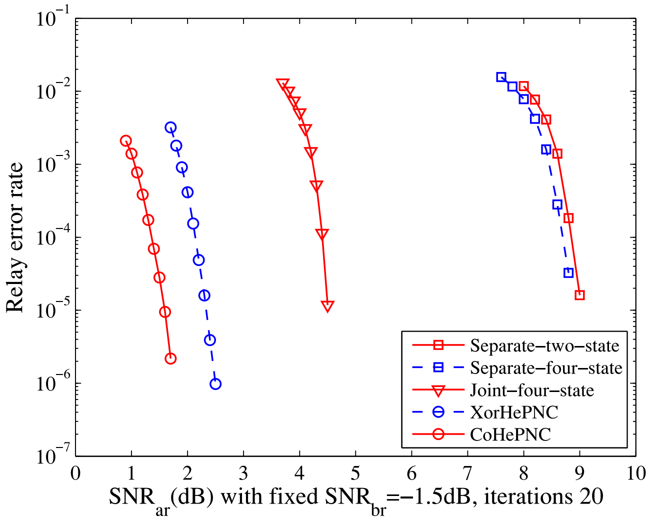

Fig. 5. Comparison of several decoding algorithms.

B. Error Performance Under Gaussian Channels

We compare both of the RER and end-to-end BER performance between the CoHePNC and the XorHePNC under Gaussian channels in Fig. 6. The end-to-end BER is defined as $\text{BER}_{all} = \frac{\Pr\{\widehat{\widehat{\mathbf{u}}}_{a1} \neq \mathbf{u}_{a1}\} + \Pr\{\widehat{\widehat{\mathbf{u}}}_{a2} \neq \mathbf{u}_{a2}\} + \Pr\{\widehat{\widehat{\mathbf{u}}}_{b} \neq \mathbf{u}_{b}\}}{3}$, where $\widehat{\widehat{\mathbf{u}}}_{a1}$, $\widehat{\widehat{\mathbf{u}}}_{a2}$ and $\widehat{\widehat{\mathbf{u}}}_{b}$ are the final estimation results in the BC stage defined in (2). The number of iterations is set to be 20. The red and square curves show the RER and BER_{all} performance, respectively. Note that increasing the number of iterations further improves the RER and BER performance. Fig. 6 shows the error performance of CoHePNC and XorHePNC with different SNR_{ar} and SNR_{br} settings. In Fig. 6(a), (b) and (c), SNR_{br} are fixed to be -0.8 dB, -1.0 dB and -1.2 dB, respectively, and SNR_{ar} are gradually increasing. In Fig. 6(a), the error performance of CoHePNC is improved with the increase of SNR_{ar} monotonously. However, for XorHePNC, the error performance is firstly improved with the increase of SNR_{ar} and then deteriorated and it reaches the worst at $\Delta\text{SNR} = \text{SNR}_{ar} - \text{SNR}_{br} = 3$ dB. Because when ΔSNR equals 3 dB as explained in Fig. 3, the SFS effects happen, which greatly reduce the error performance of relay decoding without a proper mapping function design. CoHePNC can deal with the SFS effects with the bit-level adaptive mapping design as the relay selects an appropriate mapping function by minimizing the errors happened in the MA stage. Fig. 6(a), (b) and (c) show the trend with different SNR_{br}

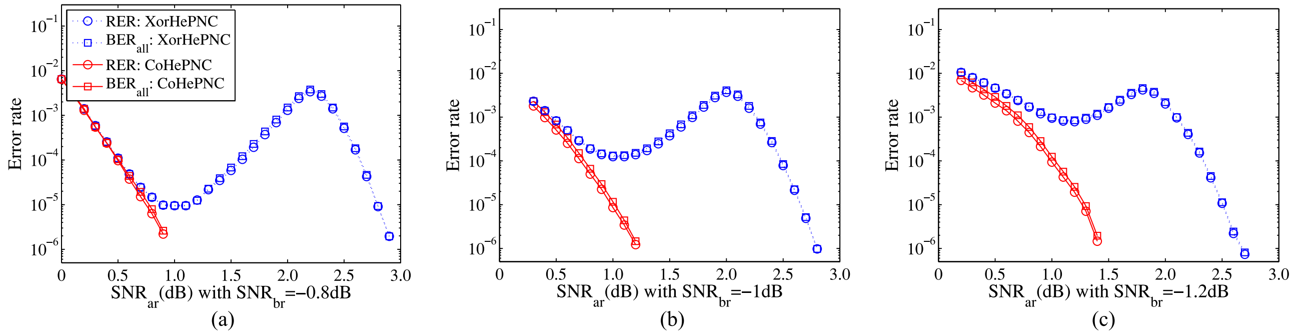

Fig. 6. CoHePNC vs XOR HePNC with codeword length 4096 bits, iterations = 20 and duplicate q = 3 under Gaussian channels. (a) $\text{SNR}_{br} = -0.8$ dB, (b) $\text{SNR}_{br} = -1.0$ dB, (c) $\text{SNR}_{br} = -1.2$ dB.

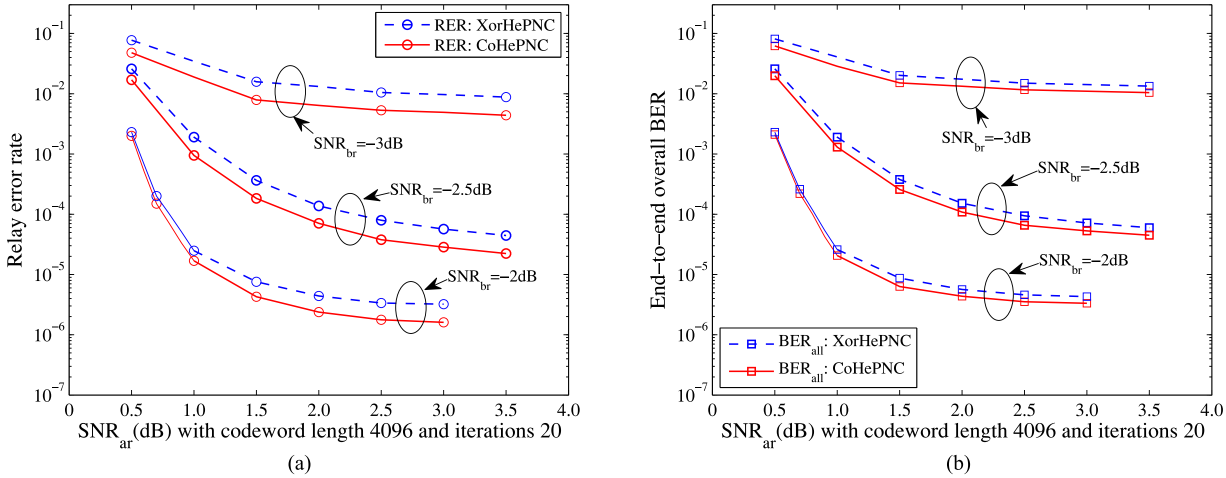

Fig. 7. CoHePNC vs XOR HePNC with iterations = 20, duplicate q = 3 under fast Rayleigh fading channels. (a) Relay error rate. (b) End-to-end BER.

settings. We can observe that when $\Delta\text{SNR} = 3$ dB, there are always inflexion points for XorHePNC due to the SFS effects.

C. Error Performance Under Fast Rayleigh Fading Channels

In the following, we compare the error performance of CoHePNC and XorHePNC under both fast and block Rayleigh fading channels. We study the error performance under the fast Rayleigh fading channels in this subsection, and the error performance under the block Rayleigh fading channels are studied in the next subsection. For the fast Rayleigh fading channels, the channel condition varies with each symbol duration. For the block Rayleigh fading channels, the channel remains the same during each codeword duration, and varies during different codeword durations. Note that for the fast Rayleigh fading channel setting, which is equivalent to that an ideal interleaver is further applied which interleaves all the bits among an infinite number of codewords. For the block Rayleigh fading channel setting, which is equivalent to without interleaver further applied among different codewords, and the interleaver only functions within each of the codeword. Note that the error floors in the following figures are caused and determined by the fixed SNR_{br} (dB), as when SNR_{ar} (dB) is sufficiently large, the RER and BER performance are bounded by the SNR_{br} of the bottleneck link L_{br}.

Fig. 7 shows the error performance of CoHePNC and XorHePNC under fast Rayleigh fading channels with the number of iterations 20. Fig. 7(a) and (b) show the RER and end-to-end BER error performance, respectively. In Fig. 7(a), we have SNR_{br} equal -3 dB, -2.5 dB and -2 dB, respectively, and gradually increase SNR_{ar}. We can observe that with the increase of SNR_{ar}, both the RER and end-to-end BER performance improve and finally converge to certain values determined by SNR_{br}. When SNR_{ar} is small, e.g., $\text{SNR}_{ar} = 0.5$ dB in Fig. 7(a), the error performance of CoHePNC and XorHePNC are similar, because given SNR_{br}, a smaller SNR_{ar} means a smaller ΔSNR and a relatively larger γ. Thus, both of CoHePNC and XorHePNC may select mapping function $\mathcal{C}3$, so they have a similar error performance. Given SNR_{br}, and with the increase of SNR_{ar}, γ reduces and the mapping function XOR is on longer suitable. Thus, CoHePNC outperforms XorHePNC with the increase of SNR_{ar}. Fig. 7(b) compares the end-to-end BER performance. For a fair comparison, the CoHePNC and XorHePNC share exactly the same BC stage setting. We can see that CoHePNC outperforms XorHePNC given the better performance of the MA stage.

Fig. 8(a) and (b) show the error performance with number of iterations 30. Compared with Fig. 7, we can observe that by increasing the number of iterations, both the RER and

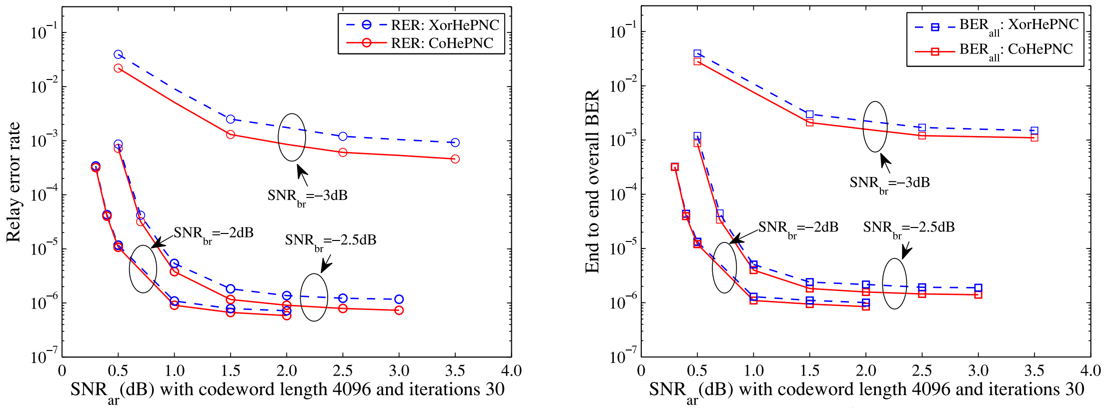

(a) (b)

Fig. 8. CoHePNC vs XOR HePNC with iterations = 30, duplicate q = 3 under fast Rayleigh fading channels. (a) Relay error rate. (b) End-to-end BER.

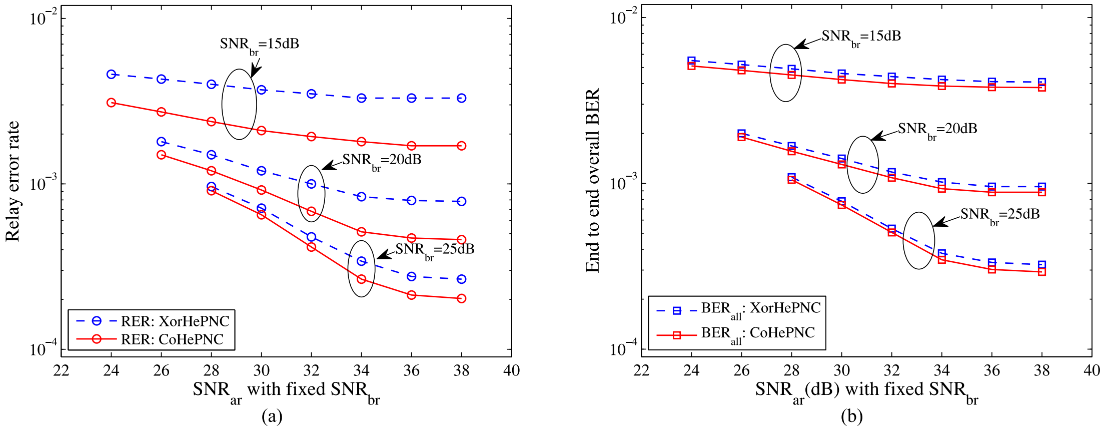

(a) (b)

Fig. 9. Block fading channel with codeword length 4096 and iterations 20. (a) Relay error rate. (b) End-to-end BER.

end-to-end BER performance converge more quickly, and the final converged performance determined by SNR$_{br}$ also improves. Note that, the error performance of CoHePNC still outperforms that of XorHePNC. Generally speaking, increasing the number of the iterations can improve the error performance because the messages at the information nodes may not be converged given a smaller number of iterations. Thus, there is a tradeoff between the complexity and the error performance. Note that, after the messages at the information nodes are converged, further increasing the number of the iterations will not improve the error performance.

D. Error Performance Under Block Rayleigh Fading Channels

In this subsection, we study the error performance of CoHePNC and XorHePNC under block Rayleigh fading channels. Fig. 9(a) and (b) show the RER and end-to-end BER performance, respectively. The codeword length is set to be 4096 bits with the number of iterations 20. We set SNR$_{br}$ to be 15 dB, 20 dB and 25 dB, respectively, and SNR$_{ar}$ are gradually increased. Note that the error performance under block Rayleigh fading channels is much worse than that of the fast Rayleigh fading channel because a fast Rayleigh fading channel is equivalent to the case with an ideal interleaver applied among an infinite number of codewords. In Fig. 9, we can observe that the error performance converge with the increase of SNR$_{ar}$ and the converge value is determined by SNR$_{br}$. When SNR$_{br}$ is small, e.g., SNR$_{br}$ = 15 dB, the improvement of CoHePNC is larger than that when SNR$_{br}$ = 25 dB, because the case of SNR$_{br}$ = 15 dB has a relatively larger ΔSNR comparing to the case SNR$_{br}$ = 25 dB, and CoHePNC outperforms XorHePNC more with a larger ΔSNR.

Note that, an interleaver may be further applied among the codewords, which will improve the error performance. In sub-Section V-C, we have studied the upper bound performance of CoHePNC with an ideal interleaver among the codewords. In this subsection, it studies the lower bound error performance that no interleaver between the codewords is further applied. In practical channels, how fast the channel changes depends on the coherent time, and the system also needs to determine whether an interleaver among codewords is applied, and how many codewords are interleaved.

VI. Conclusion

In this paper, we proposed the CoHePNC scheme under the asymmetric TWRC scenario, which integrates channel error control coding into HePNC in a link-to-link coding. The key issues in CoHePNC design are how to obtain the raw decoding results from the superimposed codewords at the relay and how to construct the network-coded sequence which contains necessary information of the source data at sources from the raw decoding results by the proper mapping functions. We proposed a full-state sum-product decoding algorithm, which utilized the full received channel information to decode the superimposed codewords to raw decoding result firstly, followed by obtained the network-coded sequence by properly designing the bit-level adaptive mapping functions. Extensive simulations are conducted and demonstrated the substantial performance gain of the proposed CoHePNC compared with the existing decoding algorithms targeting for symmetric PNC under both Gaussian and Rayleigh fading channels.

References

[1] S. Zhang, S. C. Liew, and P. P. Lam, "Hot topic: physical-layer network coding," in *Proc. 12th Annu. Int. Conf. Mobile Comput. Netw.*, 2006, pp. 358–365.

[2] P. Popovski and H. Yomo, "The anti-packets can increase the achievable throughput of a wireless multi-hop network," in *Proc. IEEE Int. Conf. Commun.*, 2006, pp. 3885–3890.

[3] S. C. Liew, S. Zhang, and L. Lu, "Physical-layer network coding: Tutorial, survey, and beyond," *Phys. Commun.*, vol. 6, pp. 4–42, Mar. 2013.

[4] M. P. Wilson, K. Narayanan, H. D. Pfister, and A. Sprintson, "Joint physical layer coding and network coding for bidirectional relaying," *IEEE Trans. Inf. Theory*, vol. 56, no. 11, pp. 5641–5654, Nov. 2010.

[5] B. Nazer and M. Gastpar, "Reliable physical layer network coding," *Proc. IEEE*, vol. 99, no. 3, pp. 438–460, Mar. 2011.

[6] W. Nam, S. Y. Chung, and Y. H. Lee, "Capacity of the Gaussian two-way relay channel to within 1/2 bit," *IEEE Trans. Inf. Theory*, vol. 56, no. 11, pp. 5488–5494, Nov. 2010.

[7] C. Cheng, J. Lee, T. Jiang, and T. Takagi, "Security analysis and improvements on two homomorphic authentication schemes for network coding," *IEEE Trans. Inf. Forensics Security*, vol. 11, no. 5, pp. 993–1002, May 2016.

[8] C. Cheng and T. Jiang, "An efficient homomorphic MAC with small key size for authentication in network coding," *IEEE Trans. Comput.*, vol. 62, no. 10, pp. 2096–2100, Oct. 2013.

[9] X. Li, T. Jiang, S. Cui, J. An, and Q. Zhang, "Cooperative communications based on rateless network coding in distributed MIMO systems," *IEEE Wireless Commun.*, vol. 17, no. 3, pp. 60–67, Jun. 2010.

[10] Y. Fan, Y. Jiang, H. Zhu, J. Chen, and X. Shen, "Network coding based privacy preservation against traffic analysis in multi-hop wireless networks," *IEEE Wireless Commun.*, vol. 10, no. 3, pp. 834–843, Dec. 2011.

[11] Y. Fan, Y. Jiang, H. Zhu, and X. Shen, "PIE: Cooperative peer-to-peer information exchange in network coding enabled wireless networks," *IEEE Wireless Commun.*, vol. 9, no. 3, pp. 945–950, Mar. 2010.

[12] P. Popovski and H. Yomo, "Physical network coding in two-way wireless relay channels," in *Proc. IEEE Int. Conf. Commun.*, Jun. 2007, pp. 707–712.

[13] S. Zhang and S.-C. Liew, "Channel coding and decoding in a relay system operated with physical-layer network coding," *IEEE J. Sel. Areas Commun.*, vol. 27, no. 5, pp. 788–796, Jun. 2009.

[14] D. Wubben and Y. Lang, "Generalized sum-product algorithm for joint channel decoding and physical-layer network coding in two-way relay systems," in *Proc. IEEE Global Telecommun. Conf.*, Dec. 2010, pp. 1–5.

[15] A. K. Tanc, T. M. Duman, and C. Tepedelenlioglu, "Design of LDPC codes for two-way relay systems with physical-layer network coding," *IEEE Commun. Lett.*, vol. 17, no. 12, pp. 2356–2359, Dec. 2013.

[16] P. Chen, Y. Fang, L. Wang, and F. C. M. Lau, "Decoding generalized joint channel coding and physical network coding in the LLR domain," *IEEE Signal Process. Lett.*, vol. 20, no. 2, pp. 121–124, Feb. 2013.

[17] X. Wu, C. Zhao, and X. You, "Joint LDPC and physical-layer network coding for asynchronous bi-directional relaying," *IEEE J. Sel. Areas Commun.*, vol. 31, no. 8, pp. 1446–1454, Aug. 2013.

[18] T. Huang, T. Yang, J. Yuan, and I. Land, "Design of irregular repeat-accumulate coded physical-layer network coding for Gaussian two-way relay channels," *IEEE Trans. Commun.*, vol. 61, no. 3, pp. 897–909, Mar. 2013.

[19] D. To and J. Choi, "Convolutional codes in two-way relay networks with physical-layer network coding," *IEEE Trans. Wireless Commun.*, vol. 9, no. 9, pp. 2724–2729, Sep. 2010.

[20] U. Bhat and T. M. Duman, "Decoding strategies at the relay with physical-layer network coding," *IEEE Trans. Wireless Commun.*, vol. 11, no. 12, pp. 4503–4513, Dec. 2012.

[21] Q. Yang and S. C. Liew, "Asynchronous convolutional-coded physical-layer network coding," *IEEE Trans. Wireless Commun.*, vol. 14, no. 3, pp. 1380–1395, Mar. 2015.

[22] D. Wubben, "Joint channel decoding and physical-layer network coding in two-way QPSK relay systems by a generalized sum-product algorithm," in *Proc. 7th Int. Symp. Wireless Commun. Syst.*, Sep. 2010, pp. 576–580.

[23] L. Yang, T. Yang, J. Yuan, and J. An, "Achieving the near-capacity of two-way relay channels with modulation-coded physical-layer network coding," *IEEE Trans. Wireless Commun.*, vol. 14, no. 9, pp. 5225–5239, Sep. 2015.

[24] T. Koike-Akino, P. Popovski, and V. Tarokh, "Adaptive modulation and network coding with optimized precoding in two-way relaying," in *Proc. IEEE Global Telecommun. Conf.*, 2009, pp. 1–6.

[25] H. Zhang, L. Zheng, and L. Cai, "Design and analysis of heterogeneous physical layer network coding," *IEEE Trans. Wireless Commun.*, vol. 15, no. 4, pp. 2484–2497, Apr. 2016.

[26] T. Koike-Akino, P. Popovski, and V. Tarokh, "Optimized constellations for two-way wireless relaying with physical network coding," *IEEE J. Sel. Areas Commun.*, vol. 27, no. 5, pp. 773–787, Jun. 2009.

[27] V. Muralidharan, V. Namboodiri, and B. Rajan, "Wireless network-coded bidirectional relaying using Latin squares for M-PSK modulation," *IEEE Trans. Inf. Theory*, vol. 59, no. 10, pp. 6683–6711, Oct. 2013.

[28] Z. Chen, H. Liu, and W. Wang, "A novel decoding-and-forward scheme with joint modulation for two-way relay channel," *IEEE Commun. Lett.*, vol. 14, no. 12, pp. 1149–1151, Dec. 2010.

[29] Z. Chen, H. Liu, and W. Wang, "On the optimization of decode-and-forward schemes for two-way asymmetric relaying," in *Proc. IEEE Int. Conf. Commun.*, 2011, pp. 1–5.

[30] Z. Chen and H. Liu, "Spectrum-efficient coded modulation design for two-way relay channels," *IEEE J. Sel. Areas Commun.*, vol. 32, no. 2, pp. 251–263, Feb. 2014.

[31] Y. Huang, S. Wang, Q. Song, L. Guo, and A. Jamalipour, "Synchronous physical-layer network coding: A feasibility study," *IEEE Trans. Wireless Commun.*, vol. 12, no. 8, pp. 4048–4057, Aug. 2013.

[32] S. ten Brink and G. Kramer, "Design of repeat-accumulate codes for iterative detection and decoding," *IEEE Trans. Signal Process.*, vol. 51, no. 11, pp. 2764–2772, Nov. 2003.

[33] D. Divsalar, H. Jin, and R. J. McEliece, "Coding theorems for "turbo-like" codes." in *Proc. Annu. Allerton Conf. Commun. Control Comput.*, 1998, pp. 201–210.

[34] F. Kschischang, B. Frey, and H.-A. Loeliger, "Factor graphs and the sum-product algorithm," *IEEE Trans. Inf. Theory*, vol. 47, no. 2, pp. 498–519, Feb. 2001.

[35] B. Nazer and M. Gastpar, "Computation over multiple-access channels," *IEEE Trans. Inf. Theory*, vol. 53, no. 10, pp. 3498–3516, Oct. 2007.

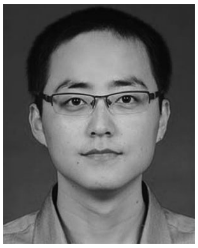

Haoyuan Zhang (S'14) received the B.S. and M.S. degrees from the Department of Electrical and Information Engineering, Harbin Institute of Technology, Harbin, China, in 2010 and 2012, respectively, and the Ph.D. degree from the Department of Electrical and Computer Engineering, University of Victoria, Victoria, BC, Canada, in 2017. His current research interests include channel error control coding, modulation optimizations, physical-layer network coding, and Massive MIMO communications.

Lin Cai (S'00–M'06–SM'10) received the M.A.Sc. and Ph.D. degrees in electrical and computer engineering from the University of Waterloo, Waterloo, ON, Canada, in 2002 and 2005, respectively. Since 2005, she has been a Professor in the Department of Electrical and Computer Engineering, University of Victoria, Victoria, BC, Canada. Her research interests include communications and networking, with a focus on network protocol and architecture design supporting emerging multimedia traffic over wireless, mobile, *ad hoc*, and sensor networks. She received the NSERC Discovery Accelerator Supplement Grants in 2010 and 2015, respectively, and the best paper awards of IEEE ICC 2008 and IEEE WCNC 2011. She has served as a TPC symposium Co-Chair for IEEE Globecom'10 and Globecom'13, an Associate Editor for IEEE Transactions on Wireless Communications, IEEE Transactions on Vehicular Technology, *EURASIP Journal on Wireless Communications and Networking*, *International Journal of Sensor Networks*, and *Journal of Communications and Networks*, and a Distinguished Lecturer of IEEE VTS society.